Discovery of small-molecule targeting the CCL20/CCR6 axis as first-in-class inhibitors for inflammatory bowel diseases

European Journal of Medicinal Chemistry xxx (xxxx) 114703

Contents lists available at ScienceDirect

European Journal of Medicinal Chemistry

journal homepage: www.elsevier.com/locate/ejmech

Research paper

Discovery of small-molecules targeting the CCL20/CCR6 axis as first-in-class inhibitors for inflammatory bowel diseases

Maria Grazia Martina [a, 1], Carmine Giorgio [a, 1], Marika Allodi [a], Simone Palese [a], Elisabetta Barocelli [a], Vigilio Ballabeni [a], Martyna Szpakowska [b], Andy Chevigne [b], Jan Piet van Hamburg [c], Nadine Davelaar [c], Erik Lubberts [c], Simona Bertoni [a, **], Marco Radi [a, *]

[a] Dipartimento di Scienze Degli Alimenti e Del Farmaco, Università Degli Studi di Parma, Viale Delle Scienze, 27/A, 43124, Parma, Italy
[b] Immuno-Pharmacology and Interactomics, Department of Infection and Immunity, Luxembourg Institute of Health, 4354, Esch-sur-Alzette, Luxembourg
[c] Department of Rheumatology, Erasmus MC, University Medical Center, Rotterdam, the Netherlands

ARTICLE INFO

Article history:
Received 12 July 2022
Received in revised form 18 August 2022
Accepted 19 August 2022

Keywords:
CCL20/CCR6
IBDs
Chemotaxis
TNBS-induced colitis
Peritonitis
Small-molecules

ABSTRACT

The CCL20/CCR6 axis is implicated in the migration of CCR6+ immune cells towards CCL20, its sole ligand, whose expression is increased during inflammatory processes and is known to play a pivotal role in triggering different autoimmune-mediated inflammatory diseases. Herein, we report a drug discovery effort focused on the development of a new pharmacological approach for the treatment of inflammatory bowel diseases (IBDs) based on small-molecule CCR6 antagonists. The most promising compound **1b** was identified by combining *in silico* studies, sustainable chemistry and *in vitro* functional/targeted assays, and its efficacy was finally validated in a classic murine model of colitis (TNBS-induced) and in a model of peritonitis (zymosan-induced). These data provide the proof of principle that a pharmacological modulation of the CCL20/CCR6 axis may indeed represent the first step for the development of an orally bioavailable drug candidate for the treatment of IBD and, potentially, other diseases regulated by the CCL20/CCR6 axis.

1. Introduction

Chemokines are small potent chemoattractant cytokines that play a pivotal role in directing the movement of immune cells through the body thanks to their binding to different chemokine receptors expressed on the leukocyte membrane. More than 20 different chemokine receptors (canonical and atypical) and over 45 different ligands have been described in the literature [1] and there is considerable cross-talk within this network as many chemokines are able to bind multiple receptors and, conversely, receptors can bind multiple ligands. This promiscuity and redundancy are the reason why these important chemokine targets have met so far very limited success in delivering new drugs to the market [2]. From this point of view, although small molecule chemokine receptor antagonists have failed to demonstrate clinical efficacy in inflammatory diseases [3], the receptor CCR6 and its ligand CCL20 are a rare example of an exclusive ligand-receptor relationship in both human and mouse, and represent therefore the ideal target for drug discovery investigations [4,5]. From a physio-pathological point of view, CCL20 is released significantly by immune and epithelial cells in inflammatory conditions and is involved in peripheral and mucosal immune responses, promoting the recruitment of CCR6$^+$ immune cells towards effector sites [6]. As a result, the CCL20/CCR6 axis is purportedly implicated in the pathogenesis of several autoimmune diseases, characterized by the altered migration and infiltration of leukocytes into different types of tissues, like skin in psoriasis, joints in rheumatoid arthritis, the central nervous system in multiple sclerosis and the gut in inflammatory bowel diseases (IBDs) [7].

In particular, although the precise etiology of IBDs is still poorly defined [8], a central role is played by the continuous recruitment of leukocytes from the circulation to inflamed tissues, also mediated by the CCL20/CCR6 pathway. Indeed, the expression of both CCR6 and its partner chemokine CCL20 is reported to be dysregulated in the colonic mucosa and serum of IBD patients [9–11] and their coding genes are considered as susceptibility genes for IBD [12]. The key pro-inflammatory role of the CCL20/CCR6 axis in IBD is further supported by a series of preclinical and clinical studies showing that: *i)* anti-CCL20

* Corresponding author.
** Corresponding author.
E-mail addresses: simona.bertoni@unipr.it (S. Bertoni), marco.radi@unipr.it (M. Radi).
[1] These authors equally contributed to the present work.

https://doi.org/10.1016/j.ejmech.2022.114703
0223-5234/© 20XX

neutralizing antibodies were able to protect against TNBS-induced colitis, preventing neutrophils and T cells infiltration in the colon [13]; *ii)* DSS-induced colitis was less severe in CCR6-knockout mice [14]; *iii)* agents indirectly decreasing serum CCL20 levels apparently have a therapeutic efficacy in IBD [15]. Overall, these data strongly suggest that the CCL20/CCR6 axis is directly involved in IBD pathogenesis and its modulation by small-molecules may represent an innovative and highly sought therapeutic approach for IBD patients. In fact, the tolerability and efficacy of current drugs (aminosalicylates, corticosteroids, immunosuppressive agents and monoclonal antibodies) is limited, and a substantial number of IBD patients fail to respond (40–55%) or to fully remit (65–80%), while respondents can lose response over time [16]. Moreover, the use of immunosuppressive and anti-TNF agents may induce lymphoma and serious opportunistic infections. Therefore, a number of small-molecules are currently under preclinical and clinical development to identify new drugs able to maintain high efficacy and limited side effects in all IBD patients [17,18]. In this picture, the chemokine receptor CCR6 has long been considered a highly desirable target for anti-inflammatory drug discovery purposes, but only a few small-molecule CCR6 antagonists have been identified so far: to the best of our knowledge, 1,4-trans-cyclohexane derivatives (e.g. Cpd35, Fig. 1) are the only CCR6 antagonists reported in a scientific journal [19], while other four chemotypes (general structures I-IV) [20–23] have been patented by major Pharma Companies (Fig. 1). However, none of these compounds has been approved for the treatment of diseases linked to the CCL20/CCR6 axis and their application in the field of IBDs has never been pursued or claimed for.

Based on the above premises, herein we report the combination of virtual library generation, docking studies on a CCR6 homology model, sustainable synthesis, *in vitro* functional assays and *in vivo* murine studies in a classic model of intestinal inflammation (TNBS-induced colitis) and in a model of acute inflammation (zymosan-induced peritonitis), to get a proof of principle on the druggability of the CCL20/CCR6 axis for the treatment of IBDs.

2. Results and discussion

It is well known that, besides the signalling promiscuity, other major hurdles to the identification of drugs targeting the chemokine system are represented by the reductionist target-based assays to screen modulators of a complex intracellular signaling and by the lack of efficacy in significant *in vivo* models, we decided to combine *in silico* target-based drug design (CCR6 antagonist) and *in vitro* functional assays (blockage of CCL20-induced chemotaxis) to identify new small molecules acting on the CCL20/CCR6 axis and get a proof of principle in a mice model of IBD. It is in fact difficult to predict the specific molecular mechanism of action (MMOA) that a first-in-class drug must trigger to change a disease phenotype and the advantages presented by the phenotypic drug discovery (PDD) could benefit from *in silico* selection of molecules based on a targeted MMOA hypothesis. This approach reminds what John Moffat named "mechanistic-informed PDD" (MIPDD): the identification of inhibitors of known or hypothesized molecular targets by assessing their effects on a therapeutically relevant phenotype [24].

At the time this study started, no X-Ray structure of CCR6 was available for *in silico* drug design and only recently a cryo-electron microscopy (cryo-EM) structure of the human chemokine receptor CCR6 bound to CCL20 and G_o protein has been published by Pfizer, giving important insights on the mechanism of activation of this peculiar GPCR [25]. To make a mechanistic-informed selection of potential disruptors of the CCL20/CCR6 axis, we relied therefore on the homology model of CCR6 in its inactive conformation available at the GPCR database (GPCRdb) [26]. Then, instead of using widespread commercial libraries of compounds for the *in silico* selection, we decided to build a large virtual collection of synthetically accessible derivatives based on two dif-

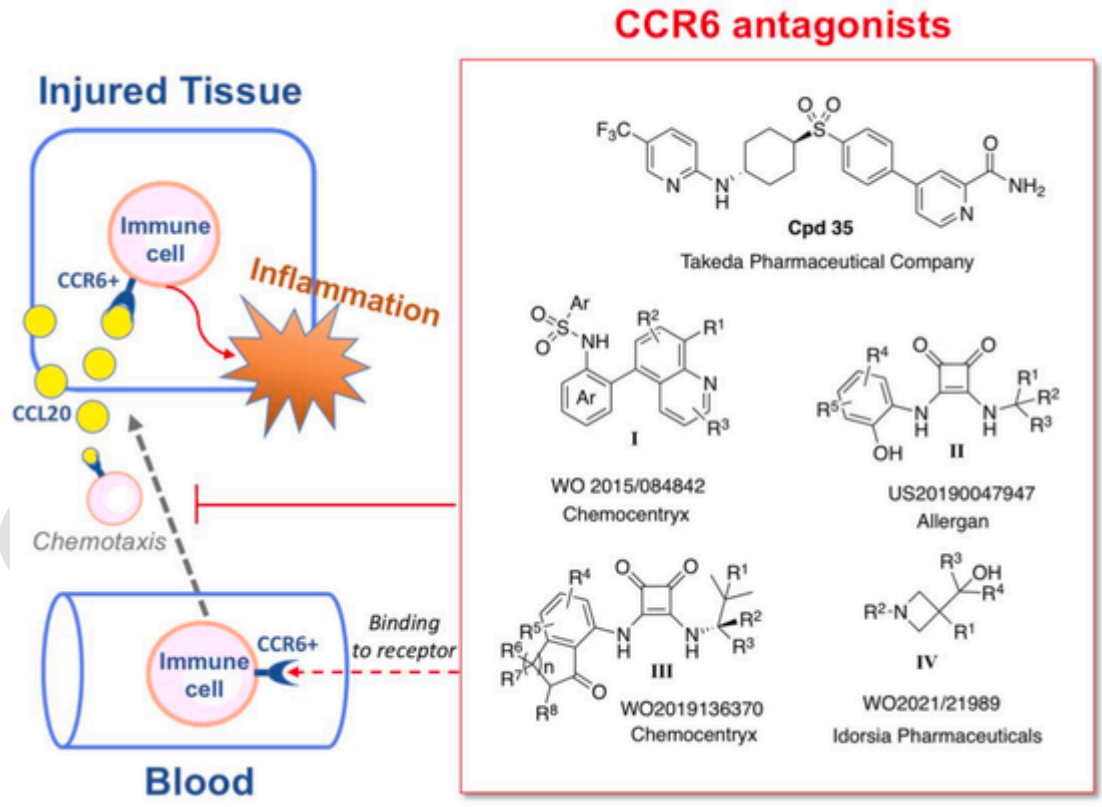

Fig. 1. Graphical representation of the CCL20-induced chemotaxis of CCR6 + immune cells and chemical structure of known CCR6 antagonists blocking immune cells chemotaxis.

ferent multicomponent synthetic protocols previously set-up by our group (MCR-1 [27] and MCR-2 [28], Scheme 1) to synthesize highly functionalized benzofurane (**1**) and hydrazone (**2**) derivatives. In detail, using MCR-1 and MCR-2 as input reactions, a series of suitable building blocks (phenols + amines for MCR-1; aldehyde or ketones + 2-chloro heterocycles for MCR-2) available in our stockroom were combined by the software SmiLib v2.0.18 [29] to generate a virtual collection of ~10000 fragment-size synthetically accessible derivatives around chemotypes **1** and **2**.

Despite the fact that docking studies cannot predict ligand affinities with high accuracy [30], they represent a very useful tool to filter out unlikely ligands and select the most promising compounds for preliminary biological evaluations. All virtual compounds were thus docked on the orthosteric site located on the extracellular part of CCR6, using the known CCR6 antagonist Cpd35 as a reference molecule to compare predicted binding modes and affinities. As shown in Fig. 2A, docking simulations on Cpd35 showed two high affinity binding poses: 1) bound to the chemokine recognition sites 1 (CRS1), in the lower energy binding pose; and 2) bound to the chemokine recognition sites 2 (CRS2). The docking poses of the top 50 ranked molecules were visually inspected, and molecules binding CRS1 and CRS2 with a binding pose similar to Cpd35 and with the highest affinity for each chemotype were selected: compounds **1a** and **2a** were predicted as CRS2 binders while **1b** and **2b** showed higher predicted affinity for CRS1 (Fig. 2).

Following the MCR-1 protocol, compounds **1a** and **1b** were synthesized by heating a mixture of the opportune aniline, chloroacetyl chloride and 2′-hydroxacetophenone in dry DMF under microwave irradiation at 140 °C for 5 min, in the presence of Cs_2CO_3 as a base. On the

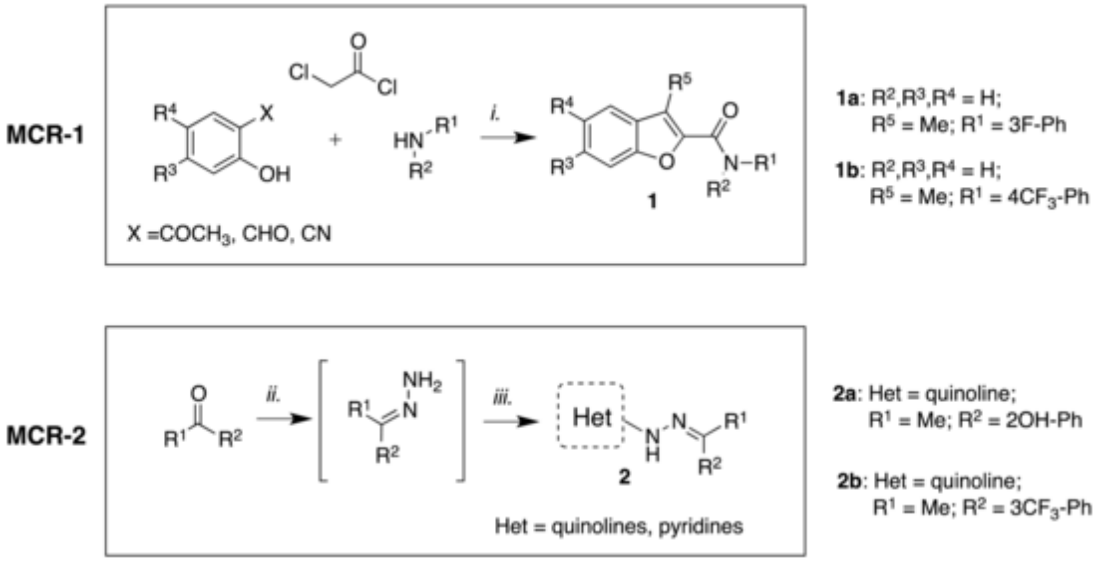

Scheme 1. *Reagents and conditions*: *i.* Cs_2CO_3, DMF, μW, 160 °C, 5 min; *ii.* hydrazine monohydrate, L-proline, toluene, μW, 300 W, 15 min; *iii.* 2-chloroquinoline, t-BuONa, $Pd(OAc)_2$, DavePhos, toluene, μW, 150 °C, 10 min.

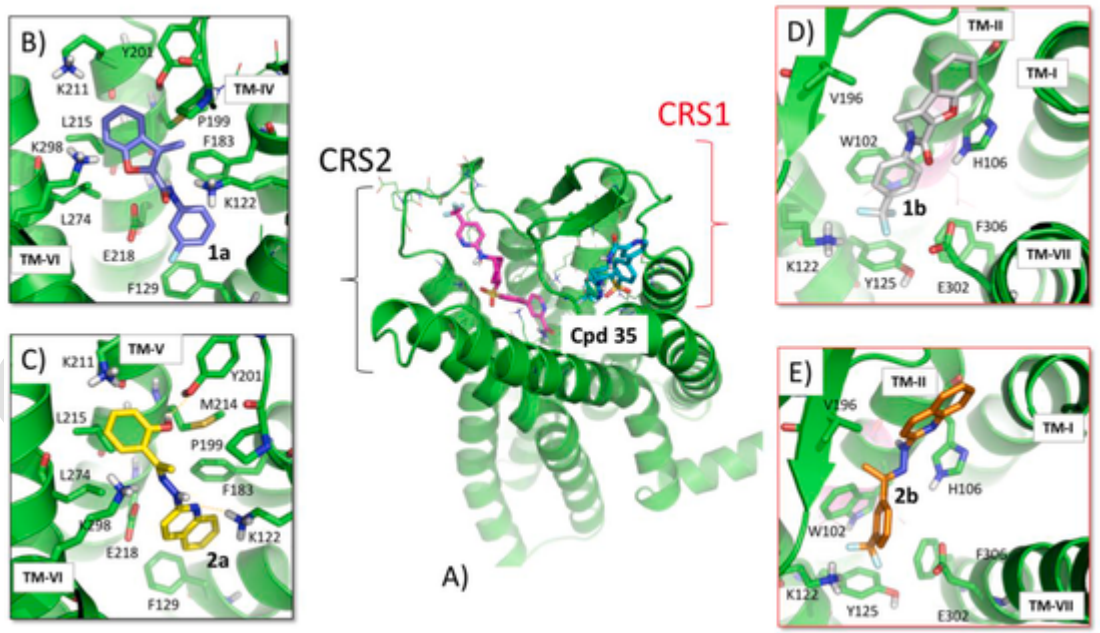

Fig. 2. Prediction of binding modes from docking studies on CCR6 homology model. A) Top ranking binding modes of Cpd35 within CRS1 and CRS2; B-E) Docking poses of top ranking compounds **1a**/**2a** within CRS2 and **1b**/**2b** within CRS1. Key residues are depicted as sticks, hydrogen bonds are reported as dotted yellow lines, TXP motif in panels E, D is reported as purple lines.

other hand, compounds **2a** and **2b** were prepared by following the MCR-2 protocol: a mixture of the opportune acetophenone and hydrazine monohydrate in toluene was irradiated at 300 W in a microwave tube for 15 min in the presence of a catalytic amount of L-proline; 2-chloroquinoline and *t*-BuONa were then added and the mixture was irradiated at 150 °C for 10 min in the presence of $Pd(OAc)_2$/DavePhos.

The cytotoxic effect of the synthesized compounds was then evaluated in $CCR6^+$ $CD4^+$ T cells obtained from 2 healthy individuals (sample 1 and 2, Fig. 3B) to determine the highest safe concentration to be used in functional assays: even if **1a,b** and **2b** did not show significative cytotoxicity up to 100 μM (Supporting information; Figs. S1–S3), we decided to use 50 μM as the maximum tolerated concentration for all compounds in the following assays. Compounds **1a,b**/**2a,b** were examined for their functional ability to suppress the CCL20-induced recruitment of $CCR6^+$ cells through a transwell chemotaxis assay: $CCR6^+CD4^+$ T cells were seeded into the upper chamber of 96-well transwell plates and 500 ng/ml CCL20 was added to the lower chamber. The CCL20-induced migration of cells towards the lower chamber was evaluated in the absence and in the presence of the compounds **1a,b**/**2a,b** (0.5-5-50 μM) incubated for 3 h (Fig. 3A). Migration index was calculated by the number of cells that migrated in response to CCL20 divided by the number of cells that migrated to the lower chamber in the absence of the chemokine (Fig. 3B). Results showed that compound **1b** was able to block the CCL20-induced $CD4^+$ T cell migration from both samples at 50 μM concentration, while compound **2b** had a similar effect only on sample 2.

Even if only a small set of molecules was evaluated, these results seem to suggest that a functional disruption of the CCL20/CCR6 axis could be achieved only by those molecules (**1b** and **2b**) targeting the minor binding pocket of CCR6 (CRS1). This hypothesis seems to be in line with the insights on the unique activation mechanism of CCR6 provided by the Pfizer cryo-EM structure [25], showing CCL20 binding only to a shallow extracellular pocket on CRS1 while other class A GPCRs require deeper agonist-binding and partial intervention of CRS2 according to the classic two-step binding mechanism of activation. In addition, the TXP motif on transmembrane domain II (TM-II) of chemokine receptor and the electrostatic charge around these residues are known to play a key role in receptor activation [31]. Thus, the predicted binding mode of **1b** to the shallow CRS1 pocket in close proximity to the TXP motif may thus account for the experimental disruption of the CCL20/CCR6 axis.

To verify that the functional effect of **1b** was due to the interaction with CCR6, a Nanoluciferase-based complementation assay was used to evaluate the β-arrestin and $miniG_i$ protein recruitment under the effect of this compound**.** In this assay, a small part of Nanoluciferase (called SmallBiT) is fused to the CCR6 receptor and the other larger part (LargeBiT) is fused to the intracellular effectors β-arrestin or miniGi, which is an engineered GTPase domain of Gα subunit. β-arrestin (or $miniG_i$) recruitment to the receptors, induced by CCL20 and/or **1b**, is monitored in HEK293T cells by NanoLuc complementation assay (NanoBiT, Promega) and can be used to quantify the effect of both agonists and antagonists. In the presence of a CCR6 agonist, β-arrestin or $miniG_i$ is recruited to the receptor, which then due do the proximity of the receptor and the effector (and so of SmBiT and LgBiT) allows Nanoluciferase complementation leading to the emission of luminescent signal directly proportional to the agonist activity of the ligand (Fig. 4A). On the other hand, testing of molecules in the antagonist mode is performed in the presence of a fixed concentration of the agonist (CCL20 at 10 nM; considered as 100% response) and the inhibitory activity of any CCR6 antagonist competing with CCL20 is expressed as percentage of the response obtained with the full agonist (Fig. 4B). As shown in Fig. 4, compound **1b** did not show any agonist effect on CCR6 at all tested concentrations but it showed a clear antagonist effect on both β-arrestin and miniGi recruitment, thus supporting the MMOA that led to the observed inhibition of chemotaxis.

Despite the great opportunity offered by CCR6 for the development of small-molecules blocking its peculiar activation mechanism triggered by CCL20, other chemokine receptors (e.g. CCR9, CXCR3, CXCR4, CCR5) have been deeply investigated for the treatment of IBDs, leading to different preclinical candidates but no approved drugs so far [32]. Since the development of highly specific ligands is generally quite challenging and considering that the inhibition of multiple targets may sometimes be planned (multi-target drug discovery) or found responsible for the desired pharmacological effect even post-approval (e.g. anticancer kinase inhibitors), we decided to evaluate the effect of compound **1b** on another target under study for IBDs: the chemokine receptor CCR5. As shown in Fig. 4, compound **1b** did not show an agonist activity but, as in the case of CCR6, it antagonized β-arrestin recruitment to CCR5 at high micromolar concentrations. However, only a few studies on the role of the CCL5/CCR5 axis in IBDs have been reported so far [33], while the CCL20/CCR6 axis can be considered a well validated approach for IBDs and its modulation with compound **1b** has provided promising functional data (Fig. 3).

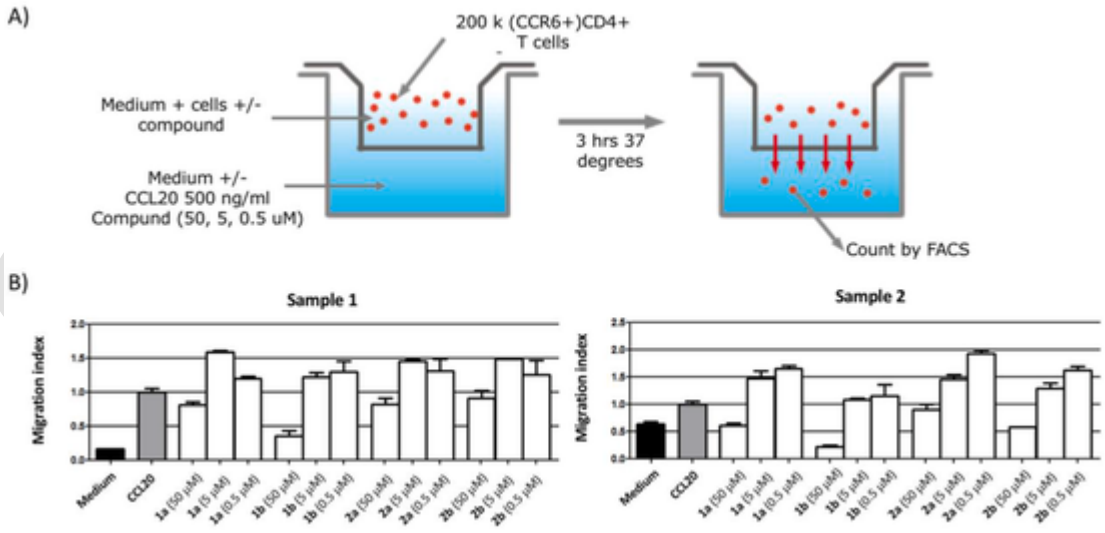

Fig. 3. Chemotaxis assay. A) Overview of the experiment set-up. B) Effect of compounds **1a,b**/**2a,b** in CCL20-induced $CCR6^+CD4^+$ T cell migration. Cells counted in combination with Count Bright absolute counting beads (Life Technologies). Medium and CCL20 (500 ng/ml) controls were tested in triplicate and compounds tested in duplicate.

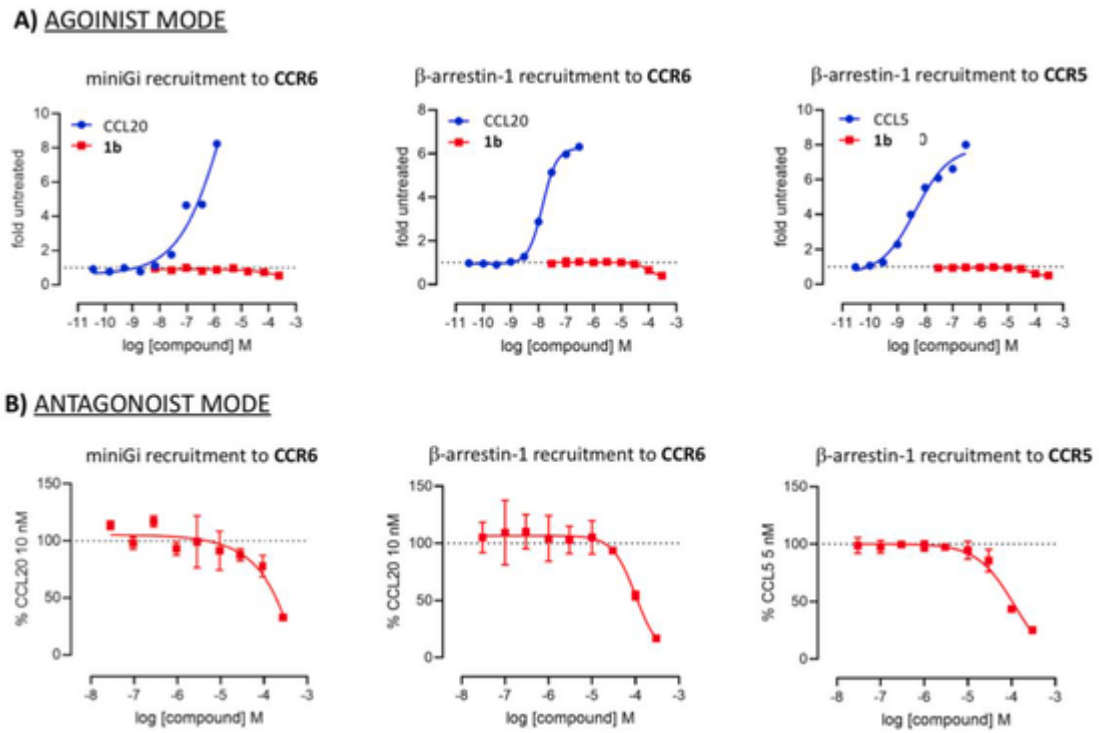

Fig. 4. Ligand-induced activity monitored by Nanoluciferase-complementation-based assays. A) miniGi recruitment to CCR6 induced by compound **1b** (30 nM–300 μM) and β-arrestin-1 recruitment to CCR6 and CCR5 induced by compound **1b** (30 nM–300 μM). CCL20 and CCL5 (30 pM–300 nM) were used as positive control (blue lines). B) Antagonist activity of compound **1b** evaluated by its ability to inhibit miniGi recruitment to CCR6 induced by CCL20 (10 nM) and β-arrestin-1 recruitment to CCR6 and CCR5 by CCL20 (10 nM) and CCL5 (5 nM), respectively.

For this reason, although compound **1b** presented a moderate activity, its clear effect in blocking the CCL20-induced chemotaxis of $CCR6^+CD4^+$ T cell prompted us to study the effect of this compound in *in vivo* models of colitis and peritonitis to get a proof of principle on its efficacy against intestinal inflammation. It is in fact known that the experimental colitis induced in mice by instillation of 2,4,6-trinitrobenzene sulfonic acid (TNBS) is characterized by increased colonic levels of CCL20 with consequent recruitment of CCR6+ immune cells and represents therefore a suitable *in vivo* model to evaluate the effect of CCL20/CCR6 modulators [12].

Colitis was thus induced in Swiss mice (n = 6–8/group) by enema (i.r.) administration of 5mg/mouse TNBS in 50% ethanol 6 days after skin sensitization. Compound **1b** at 1 mg/kg or vehicle were subcutaneously (s.c.) applied twice daily for 3 days after TNBS challenge. Sham mice received saline 50 μL i.r. and 10 mL/kg s.c. Disease Activity Index (DAI), scoring the severity of colitis, macroscopic score, expressing the degree of colonic mucosal injury, and myeloperoxidase activity (MPO) in colon and lungs, marker of leukocyte recruitment, were determined. Compared to the sham group, TNBS mice showed a significantly higher value of DAI, due to both body weight loss and softening of stools, along with a remarkable damage of the mucosa. Colonic and pulmonary myeloperoxidase (MPO) activity strongly augmented upon colitis induction, indicating a conspicuous enrolment of granulocytes within tissues. Daily treatment with compound **1b** 1 mg/kg improved mice general conditions, attenuated macroscopic injury and counteracted neutrophils infiltration, both in the colon and in lungs (Fig. 5).

Considering the promising results obtained in the TNBS-induced colitis model, we decided to assess the versatility of **1b** by evaluating its efficacy in zymosan-induced peritonitis, a model of acute inflammation linked to the CCL20/CCR6 axis [34].

Intraperitoneal injection of zymosan produced the massive recruitment of neutrophils into the peritoneal cavity (Fig. 6A), a remarkable augmentation of total proteins in the peritoneal fluid (Fig. 6B) and of myeloperoxidase activity (Fig. 6C). Compound **1b** was not able to attenuate the zymosan-induced flogistic response when administered once; however, the double treatment (1 mg/kg before and after zymosan treatment) significantly reduced the total protein content and myeloperoxidase activity in the peritoneal lavage, showing anti-inflammatory effects comparable to those of the potent agent dexamethasone, and similarly to the results collected in TNBS-induced colitis, where the protective action emerged following a double daily treatment (Fig. 6).

3. Conclusion

Up to date, a number of studies on autoimmune-mediated inflammatory disease models have demonstrated the protective effect induced by a negative interference with the CCL20/CCR6 axis, which can be achieved by administration of anti-CCL20 mAbs or using CCR6−/− mice [12–14]. Further insights in the druggability of the CCL20/CCR6 axis have been obtained by using anti-CCR6 mAbs in mouse models of experimental autoimmune encephalomyelitis (EAE) and psoriasis, resulting in the prevention of leukocytes' infiltration and attenuation of clinical symptoms [35]. However: *i)* mAbs present several drawbacks for wide clinical application; *ii)* only a few small-molecule CCR6 antagonists have been identified so far; *iii)* no CCR6 antagonists have been approved yet for the treatment of diseases linked to the CCL20/CCR6 axis; *iv)* the application of CCR6 antagonists in the field of IBDs has never been pursued or claimed for.

Up to now, only one anti-CCL20 mAb (GSK3050002), selectively inhibiting the recruitment of CCR6+ T cells, has been evaluated in phase I clinical trial while a phase II trial in psoriatic arthritis initiated in 2016 was withdrawn shortly thereafter [36,37]. Despite the fact that other anti-CCL20 mAbs are under study for different diseases connected to a dysregulation of the CCL20/CCR6 axis, major drawbacks of mAbs are their high costs, poor compliance and convenience related to the parenteral route of administration and immunogenicity after long-term treatment.

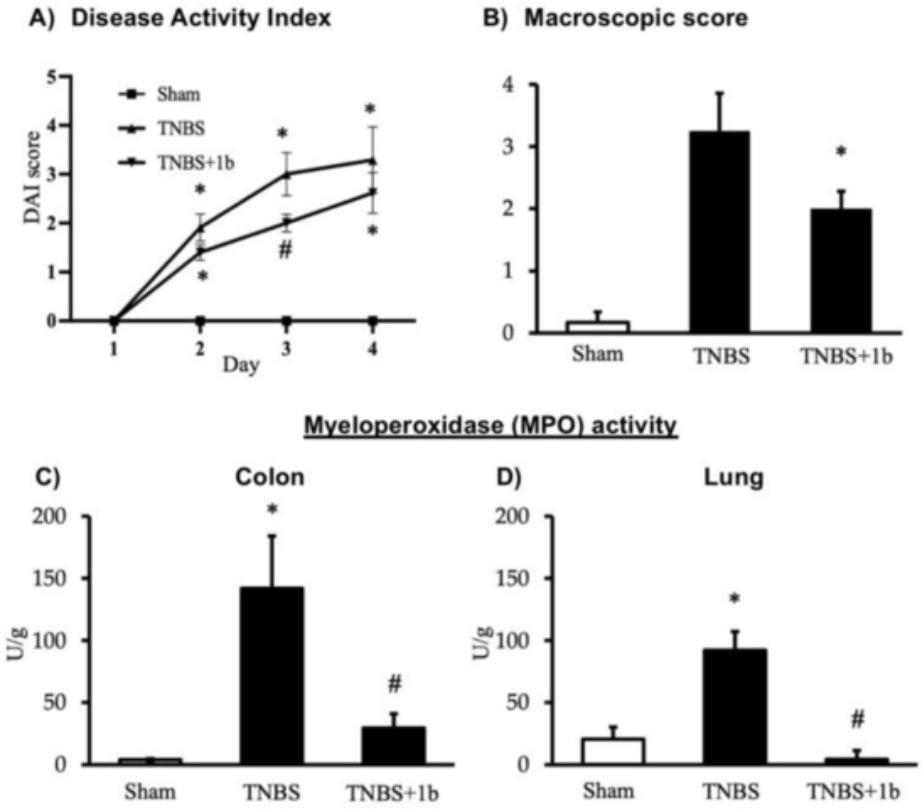

Fig. 5. Effects of compound 1b on TNBS-induced inflammatory responses. Disease Activity Index (A), macroscopic score (B), colonic MPO (C) and lung MPO (D) activity assessed in vehicle-treated sham mice (Sham) and in TNBS-treated mice administered with vehicle (TNBS) and compound **1b** 1 mg/kg (TNBS + **1b**). *P < 0.05 vs. sham mice; #P < 0.05 vs. TNBS mice; one-way or two-way ANOVA followed by Bonferroni's post-test.

Based on these premises, the present study reports the application of a mechanistic-informed PDD approach to identify novel modulators of the CCL20/CCR6 axis as first-in-class inhibitors for IBDs. Starting from a homology model of inactive CCR6, a virtual combinatorial library (VCL) of synthetically accessible derivatives (based on in house MCR protocols) has been generated and docked on the extracellular portion of CCR6. Using the known CCR6 antagonist Cpd15 as a reference for the docking studies, four top ranked compounds **1a,b/2a,b** were selected from the VCL and synthesized by application of sustainable MCR protocols. A phenotypic screening based on CCL20-induced chemotaxis of $CCR6^{+}CD4^{+}$ T cells identified compound **1b** as the most promising candidate in disrupting the CCL20/CCR6 axis by acting as antagonist of CCR6, as observed in a subsequent nanoluciferase complementation assay. Finally, the collected *in vivo* data showed that compound **1b** was able to improve health conditions and to prevent colon and systemic neutrophils recruitment in a classic murine model of colitis induced by TNBS instillation and effective in attenuating the inflammatory response triggered by zymosan intraperitoneally injected.

Considering that the TNBS-induced colitis is a subacute model of intestinal inflammation, characterized by the primary activation of the adaptive immunity [38], whereas the acute peritoneal inflammation induced by zymosan is associated with strong innate immune responses involving neutrophils chemotaxis [39], our collected data show for the first time that it is possible to use a small-molecule (**1b**) to modulate lymphocytes response and neutrophils migration by negatively interfering with the CCL20/CCR6 axis.

This work represents therefore a first step in the development of an innovative therapeutic approach for the treatment of IBDs, which may lead to an orally bioavailable drug candidate in the future. Further studies on the optimization of compound **1b** are currently ongoing and will be reported in due course.

4. Experimental section

4.1. Chemistry

General. All commercially available chemicals were purchased from Merck or Fluorochem and, unless otherwise noted, used without any previous purification. Solvents used for work-up and purification procedures were of technical grade. TLC was carried out using Merck TLC plates (silica gel on Al foils, SUPELCO Analytical). Where indicated, products were purified by silica gel flash chromatography on columns packed with Merck Geduran Si 60 (40–63 μm). ^{1}H and ^{13}C NMR spectra were recorded on BRUKER AVANCE 300 MHz and BRUKER AVANCE 400 MHz spectrometers. Chemical shifts (δ scale) are reported in parts per million relative to TMS. ^{1}H NMR spectra are reported in this order: multiplicity and number of protons; signals were characterized as: s (singlet), d (doublet), dd (doublet of doublets), ddd (doublet of doublet of doublets), t (triplet), m (multiplet), bs (broad signal). Low resolution mass spectrometry measurements were performed on quattromicro API tandem mass spectrometer (Waters, Milford, MA, USA) equipped with an external APCI or ESI ion source. ESI-mass spectra are reported in the form of (m/z). Elemental analyses were performed on a ThermoQuest (Italia) FlashEA 1112 Elemental Analyzer. All final compounds were >95% pure as determined by elemental analysis. data for C, H, and N (within 0.4% of the theoretical values).

Microwave Irradiation Experiments. Microwave reactions were conducted using a CEM Discover Synthesis Unit (CEM Corp., Matthews, NC). The machine consists of a continuous focused microwave power delivery system with an operator-selectable power output from 0 to 300 W. The temperature inside the reaction vessel was monitored using a calibrated infrared temperature control mounted under the reaction vessel. All experiments were performed

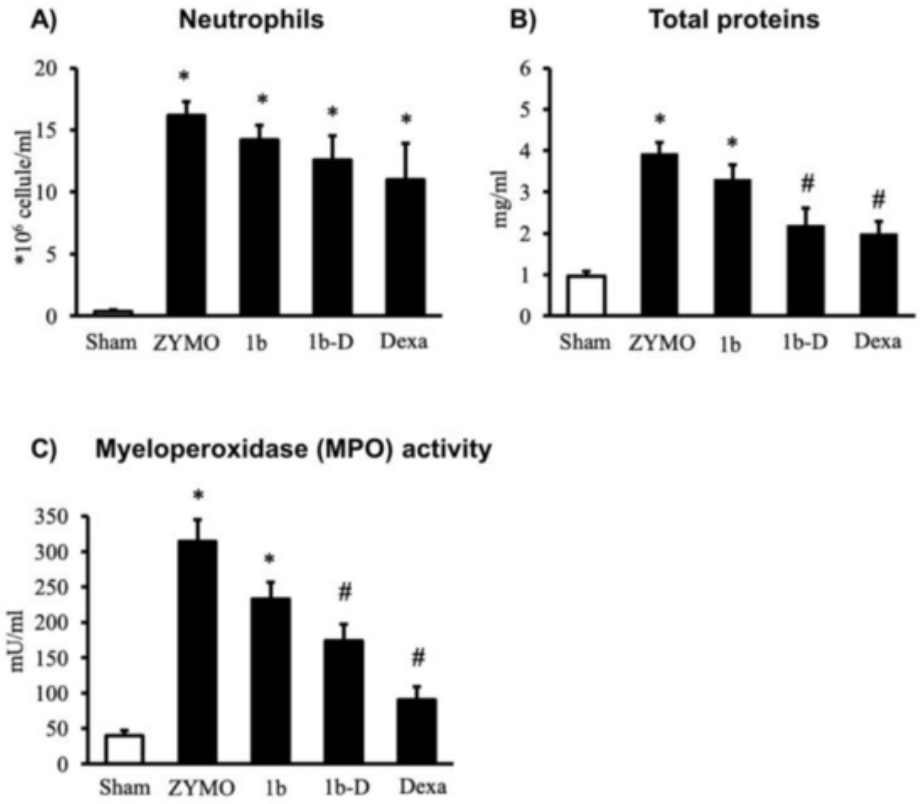

Fig. 6. Effects of compound 1b on zymosan-induced peritonitis. Neutrophils count (A), total proteins content (B) and myeloperoxidase activity (C) detected in the peritoneal lavage of vehicle-treated sham mice (Sham) and zymosan-treated mice administered with vehicle (ZYMO), compound **1b** 1 mg/kg (**1b**), compound **1b** 1 mg/kg double injection (**1b-D**), and dexamethasone 3 mg/kg (Dexa). *P < 0.05 vs. sham mice; #P < 0.05 vs. ZYMO mice; one-way ANOVA followed by Bonferroni's post-test.

using a stirring option whereby the reaction mixtures were stirred by means of a rotating magnetic plate located below the floor of the microwave cavity and a Teflon-coated magnetic stir bar in the vessel.

4.2. General procedure for the synthesis of benzofuran-2-carboxamides

In a microwave tube 3-F aniline or 4-CF_3 aniline (0.54 mmol), chloroacetyl chloride (42 μL; 0.54 mmol) and 2′-hydroxacetophenone (0.42 mmol) were added to dry DMF cooled to 0 °C. Cs_2CO_3 (439 mg, 1.35 mmol) was added and the tube was heated at 160 °C for 5 min (max μW power input: 200 W; ramp time: 1 min; reaction time: 5 min; power max: off; maximum pressure: 190 psi). At the end of the irradiation, H_2O and ethyl acetate were added. The organic phase was washed with an aqueous solution of LiCl (5%), brine, dried over Na_2SO_4 and concentrated under vacuum. The crude was purified by flash chromatography, using petroleum ether/diethyl ether 95/5 as eluent.

***N*-(3-fluorophenyl)-3-methylbenzofuran-2-carboxamide (1a):** Yield: 25%; MS (ESI) $[M+H]^+$ = 270.3 m/z, $[M+Na]^+$ = 292.4 m/z; ^{1}H NMR ($CDCl_3$ 400 MHz): δ 2.68 (s, 3H); 6.87 (t, 1H, *J* = 8 Hz); 7.35 (m, 3H); 7.49 (m, 2H); 7.65 (d, 1H, *J* = 8Hz); 7.72 (m, 1H); 8.41 (s, 1H); ^{13}C NMR ($CDCl_3$ 100 MHz): δ 9.05; 107.37; 111.59; 115.15; 121.12; 123.42; 124.30; 127.62; 130.10; 130.19; 138.97; 141.99; 153.26; 158.04; 161.84; 164.27. mp (104–105 °C).

3-methyl-*N*-(4-(trifluoromethyl)phenyl)benzofuran-2-carboxamide (1b): Yield: 30%; MS (ESI) $[M+H]^+$ = 320.3 m/z, $[M+Na]^+$ = 342.4 m/z; ^{1}H NMR ($CDCl_3$ 400 MHz): δ 2.69 (s, 3H); 7.35 (m, 1H); 7.49 (m, 2H); 7.64 (m, 3H); 7.85 (d, 2H, *J* = 9Hz); 8.49 (bs, 1H); ^{13}C NMR ($CDCl_3$ 100 MHz): δ 9.11; 111.65; 119.48; 121.23; 122.76; 123.53; 124.75; 125.76; 126.38; 127.80; 129.74; 140.59; 141.88; 153.34; 158.16. mp (164–165 °C).

4.3. General procedure for the synthesis of quinoline-hydrazone derivatives

2-hydroxy acetophenone or 3-(trifluoromethyl) acetophenone (0.73 mmol), hydrazine monohydrate (0.73 mmol), L-proline (0.15 mmol) and 1 mL of anhydrous toluene were placed in a dried 10 mL microwave tube equipped with a magnetic stir bar and a septum, and the colourless mixture was irradiated at 300 W for 15 min in the microwave apparatus (maximum pressure: 250 psi; maximum temperature: 200 °C; power max: off; stirring: on). Subsequently, 2-chloroquinoline (0.61 mmol) and t-BuONa (0.98 mmol) were added, and the tube was flushed with argon for 1 min. Then, 1 mL of a stock solution of the catalyst [$Pd(OAc)_2$ (27.0 mg; 0.12 mmol) plus DavePhos (96 mg, 0.24 mmol) in anhydrous toluene (10 mL) stored under argon atmosphere] was added and the resulting mixture was stirred and flushed with argon for additional 2 min. Next, the tube was heated under microwave irradiation at 150 °C for 10 min (max μW power input: 300 W; maximum pressure: 250 psi; power max: off; stirring: on). After cooling to room temperature, the dark red reaction mixture was filtered over celite, and the resulting solution was evaporated under reduced pressure. The residue was purified by silica gel flash chromatography from 9/1 to 7/3 petroleum ether/ethyl acetate as eluent.

(*E*)-2-(1-(2-(quinolin-2-yl)hydrazineylidene)ethyl)phenol (2a): Yield: 48%; MS (ESI) $[M+H]^+$ = 278.4 m/z; ^{1}H NMR ($CDCl_3$ 300 MHz): δ 2.44 (s, 3H); 6.93 (t, 1H, *J* = 6 Hz); 7.05 (d, 1H, *J* = 6 Hz); 7.30–7.39 (m, 4H); 7.50 (d, 1H, *J* = 6 Hz); 7.65 (t, 1H, *J* = 6 Hz); 7.74–7.76 (m, 2H); 8.11 (d, 1H, *J* = 6Hz); ^{13}C NMR ($CDCl_3$ 100 MHz): δ 29.72; 108.91; 117.47; 119.07; 119.84; 123.76; 124.93; 126.12; 127.23; 127.83; 130.37; 130.57; 139.16; 146.81; 149.65; 154.44; 158.08.

(*E*)-2-(2-(1-(3-(trifluoromethyl)phenyl)ethylidene) hydrazineyl)quinoline (2b): Yield: 65%; MS (ESI)

$[M+H]^+$ = 330.12 m/z; ^1H NMR ($CDCl_3$ 300 MHz): δ 2.25 (s, 3H); 6.92 (m, 1H); 7.32 (t, 1H, *J* = 6 Hz); 7.49 (t, 1H, *J* = 6 Hz); 7.59–7.64 (m, 2H); 7.68–7.77 (m, 2H); 7.95 (d, 1H, *J* = 6 Hz); 8.06 (m, 2H); 8.68 (bs, 1H); ^{13}C NMR ($CDCl_3$ 100 MHz): δ 29.74; 109.92; 122.43; 123.44; 124.79; 125.14; 126.04; 126.27; 127.82; 128.84; 130.00; 130.59; 131.02; 138.47; 139.39; 141.63; 147.0; 155.70.

5. Molecular modeling

The virtual combinatorial library (VCL) of compounds around MCR-1 and MCR-2 was generated with SmiLib v2.0, available as a Java executable from http://melolab.org/smilib/and enabling the combinatorial generation of structures **1** and **2** from inputted in house available building blocks. The input and output structures were encoded as SMILES. The resulting VCL of synthetically accessible derivatives was geometry optimized using the MMFF94 force field [40] (conjugated gradient, convergence criteria of 1×10^{-6} or a maximum of 5000 iterations) with OpenBabel 2.3.2 software [41]. Also, non-polar hydrogens were removed from the ligands and Gasteiger charges were assigned employing OpenBabel 2.3.2 software.

Docking studies were performed with Autodock Vina [42] through PyRx [43], while PyMol [44] was used to visualize the results. Docking runs were performed within a 70 Å × 70 Å × 70 Å cubic box surrounding the CCR6 ortosteric pocket. A search exhaustiveness of 10 was used and only conformers corresponding to the best scoring docking pose of those compounds from the VCL that achieved a ΔG docking ≤ −8.0 kcal/mol were selected.

6. Biology

6.1. In vitro assays

6.1.1. Human memory $CD4^+$ T cells

Peripheral blood mononuclear cells (PBMC) were isolated from buffy coats from healthy individuals that were obtained from Sanquin Blood Bank (Rotterdam, the Netherlands). PBMC were isolated using a Ficoll-gradient and stained with monoclonal antibodies against CD45RO (clone UCHL1), CD4 (clone RPA-T4) (all BD Biosciences, San Diego, CA, USA), CD3 (clone UCHT1) (BioLegend, San Diego, CA, USA) as appropriate in 0.5% BSA + 2 mM EDTA in PBS. From isolated PBMC, memory $CD4^+$ T cells were selected using a Memory $CD4^+$ T Cell Isolation Kit (Miltenyi Biotec) according to standard protocols. Separation of memory $CD4^+$ T cells was performed with an autoMACS Pro Separator (Miltenyi Biotec). Purity of sorted memory $CD4^+$ T cells is over 95% by this method.

6.1.2. Toxicity assay

20×10^4 memory $CD4^+$ T cells were cultured with or without different doses of CCR6 compounds (5-50-100-200-500 μM) for 3 h incubation at 37 °C and 5% CO_2. Cells were stained for annexin and propidium iodide and the percentage of viable cells were measured on a FACSCantoII Flow Cytometer.

6.1.3. Chemotaxis assay

20×10^4 memory $CD4^+$ T cells were seeded into the upper chamber of 96-well transwell plates with a 5.0 μm pore polycarbonate membrane (Corning, New York, NY, USA) in migration medium (Iscove's Modified Dulbecco's Medium supplemented with 2 mM L-glutamin, 100 U/ml penicillin/streptomycin (Lonza, Verviers, Belgium), 50 μM β-mercaptoethanol (Sigma-Aldrich, St. Louis, MO, USA), and for decreasing background migration 0.5% bovine serum albumin instead of 10% fetal calf serum). Migration medium with or without CCR6 compounds (0.5-5-50 μM) or 500 ng/ml CCL20 (R&D Systems, Minneapolis, MN, USA) was added to the lower chamber. Cells and compounds were pre-incubated for 15 min at 4°. Each condition was run in duplicate or triplicate. After 3 h incubation at 37 °C and 5% CO_2, migrated cells were counted using CountBright beads (Invitrogen, Waltham, MA, USA) on a FACSCantoII Flow Cytometer. The migration index was calculated by the number of cells that migrated in response to the chemokine divided by the number of cells that migrated to standard migration medium.

6.1.4. Nanoluciferase-based complementation assay

HEK293T cells were purchased from ATCC and were grown in DMEM +10% fetal bovine serum (FBS) and penicillin/streptomycin (100 Units/ml and 100 μg/ml). CCL20 was purchased from PeproTech. Ligand-induced β-arrestin-1 or miniGi protein recruitment to CCR6 and CCR5 was monitored by Nanoluciferase complementation assay (NanoBiT; Promega) as previously described (ref) [45–47]. HEK-293T cells were co-transfected with pNBe vectors encoding CCR6 and CCR5 C-terminally tagged with SmBiT and human β-arrestins or miniGi protein (engineered GTPase domains of Gαi subunits) [48] N-terminally tagged with LgBiT. 24 h after transfection, cells were harvested and incubated for 15 min at 37 °C with Coelenterazine h (Regis Technologies). 105 cells/well were then distributed into white 96-well plates. To evaluate agonist activity, β-arrestin and miniGi recruitment to the receptor induced by compound **1b** (30 nM–300 μM) was measured for 20 min with a Mithras LB940 microplate reader (Berthold Technologies). CCL20 (30 pM–300 nM) was used as positive control. To evaluate **1b** antagonist activity, cells were subsequently incubated with CCL20 (10 nM) or CCL5 (5 nM) and the inhibition of chemokine-induced β-arrestin and miniGi recruitment to the CCR6 and CCR5 receptors was monitored.

7. In vivo studies

7.1. Animals

All animal experiments were performed according to the guidelines for the use and care of laboratory animals and they were authorized by the local Animal Care Committee "Organismo Preposto al Benessere degli Animali" and by Italian Ministry of Health, "Ministero della Salute" (DL 26/2014). All appropriate measures were taken to minimize pain or discomfort of animals. Female CD1 Swiss mice (7–12 weeks old) (Charles River Laboratories, Calco, Italy), weighing 25–30g, were housed five per cage and maintained under standard conditions at our animal facility (12:12 h light–dark cycle, water and food *ad libitum*, 22–24 °C). All the experimental procedures (induction of colitis, zymosan-induced peritonitis) and euthanasia by CO_2 inhalation were performed between 9 a.m. and 2 p.m.

7.2. TNBS-induced colitis

Six days before intrarectal (i.r.) instillation, animals were subjected to skin sensitization through cutaneous application of 50 μL of a 10% (w/v) 2,4,6-trinitrobenzene sulfonic acid (TNBS) solution in 50% ethanol. After 20 h fasting with free access to water containing 5% glucose, colitis was induced by i.r. instillation of the same volume and concentration of TNBS applied during skin sensitization [49]. TNBS instillation was performed using a PE50 catheter, positioned 4 cm from the anus, in anaesthetized mice (isoflurane 2%) kept in the head-down position for 3 min to avoid the leakage of intracolonic instillate.

Mice were assigned through block randomization to the sham group (n = 6), i.r. inoculated with 50 μL 0.9% NaCl (saline solution) and administered s.c. 10 mL/kg vehicle (DMSO 1% in saline solution), or to the following experimental groups of colitic mice: TNBS group, receiving vehicle 10 mL/kg (n = 8); TNBS + 1b mice, receiving compound **1b** at 1 mg/kg (n = 12) Compound **1b** or the vehicle was subcutaneously administered twice daily, 8 h apart, starting from day 1, after TNBS enema, to day 4, when mice were euthanized by CO_2 inhalation.

7.2.1. Evaluation of inflammatory responses

Body weight, stools consistency and rectal bleeding were examined and registered daily throughout the experimentation by unaware observers, in order to assess the disease activity index (DAI). Immediately after euthanasia the macroscopic damage of colonic mucosa was assessed as macroscopic score. Colon and lungs were collected for subsequent myeloperoxidase activity assay.

7.2.2. Disease activity index (DAI)

DAI is a parameter that estimates the severity of the disease; it consists on the daily assignment of a total score, according to Cooper's modified method [50], on the basis of body weight loss, stool consistency and rectal bleeding. The scores were attributed blindly by two investigators and were quantified as follows: stool consistency: 0 (normal), 1 (soft), 2 (liquid); body weight loss: 0 (<5%), 1 (5–10%), 2 (10–15%), 3 (15–20%), 4 (20–25%), 5 (>25%) and rectal bleeding: 0 (absent), 1 (present).

7.2.3. Colon macroscopic damage score (MS)

After euthanasia, the colon was explanted, opened longitudinally, flushed with saline solution and MS was immediately evaluated through inspection of the mucosa, executed by two investigators unaware of the treatments applied. MS was determined according to previously published criteria (Giorgio et al., 2021), as the sum of scores (max = 14) attributed as follows: presence of strictures and hypertrophic zones (0, absent; 1, 1 stricture; 2, 2 strictures; 3, more than 2 strictures); mucus (0, absent; 1, present); adhesion areas between the colon and other intra-abdominal organs (0, absent; 1, 1 adhesion area; 2, 2 adhesion areas; 3, more than 2 adhesion areas); intraluminal hemorrhage (0, absent; 1, present); erythema (0, absent; 1, presence of a crimsoned area <1 cm [2]; 2, presence of a crimsoned area >1 cm^2); ulcerations and necrotic areas (0, absent; 1, presence of a necrotic area <0.5 cm^2; 2, presence of a necrotic area >0.5 cm^2 and <1 cm^2; 3, presence of a necrotic area >1 cm^2 and <1.5 cm^2; 4, presence of a necrotic area >1.5 cm^2).

7.2.4. Colonic and pulmonary myeloperoxidase (MPO) activity assay

MPO activity, marker of tissue granulocytic infiltration, was determined according to Ivey's modified method [51]. After being weighed, each colonic or lung sample was homogenized in ice-cold 0.02 M sodium phosphate buffer (pH 4.7), containing 0.015 M Na_2EDTA and 1% Halt Protease Inhibitor Cocktail (ThermoFisher Scientific), and centrifuged for 20 min at 12500 RCF at 4 °C. Pellets were re-homogenized in four volumes of ice-cold 0.2 M sodium phosphate buffer (pH 5.4) containing 0.5% hexadecylthrimethyl-ammoniumbromide (HTAB) and 1% Halt Protease Inhibitor Cocktail (ThermoFisher Scientific). Samples were then subjected to three cycles of freezing and thawing and centrifuged for 30 min at 15500 RCF at 4 °C. 50 μL of the supernatant was then allowed to react with 950 μL of 0.2 M sodium phosphate buffer, containing 1.6 mM tetramethylbenzidine, 0.3 mM H_2O_2, 12% dimethyl formamide, 40% Dulbecco's phosphate buffered saline (PBS). Each assay was performed in duplicate and the rate of change in absorbance was measured spectrophotometrically at 690 nm (TECAN Sunrise™ powered by Magellan™ data analysis software, Mannedorf, Switzerland). 1 unit of MPO was defined as the quantity of enzyme degrading 1 μmol of peroxide per minute at 25 °C. Data were normalized with edema values [(wet weight-dry weight) dry $weight^{-1}$] [52] and expressed as U/g of dry weight tissue.

7.3. Zymosan-induced peritonitis

The experiments were performed in mice fasted 2h before zymosan A injection, but with free access to water. Peritonitis was induced following a modification of Thurmond's method (2004), by injecting into the peritoneal space of mice 5 mg/mL zymosan A in PBS (final volume 0.2 mL). Mice were assigned through block randomization to the sham group (sham) (n = 9), i.p. injected with PBS (0.2 mL) and administered s.c. vehicle (DMSO 1% in saline solution; 10 mL/kg), or to the following experimental groups of mice, receiving subcutaneously the treatment in study, injected 1h before zymosan: control group (ZYMO), receiving vehicle 10 mL/kg s.c. (n = 19); **1b** group, receiving compound **1b** 1 mg/kg s.c. (n = 8); **1b**-D group, receiving compound **1b** 1 mg/kg administered twice s.c., 1h before and 2h after zymosan injection (n = 5); Dexa group, receiving dexamethasone 3 mg/kg s.c. (n = 5). 4h after zymosan administration, mice were euthanized: the peritoneal cavity was washed with 3 mL of PBS containing 3 mM EDTA and 25 U/ml heparin and the volume collected with automatic pipettes. The peritoneal lavage was centrifuged at 400 RCF for 15 min at 4 °C to collect the cells. The protein content of the supernatant was spectrophotometrically determined following the bicinchonate method with a commercial kit (Pierce, BCA protein assay kit) and expressed as mg/mL of the peritoneal fluid, while the pellet was used for the determination of myeloperoxidase activity, according to the method previously described and expressed as mU/mL of the peritoneal lavage, or suspended in cell staining buffer (PBS containing 0.5% fetal calf serum (FCS) and 0.1% sodium azide and subjected to flow cytometry assays.

7.3.1. Flow cytometry assays

7.3.1.1. Immunofluorescent staining. Prior to staining with antibodies, 200 μL of the suspension of peritoneal cells was incubated with IgG1-Fc (1 μg/10^6 cells) for 10 min in the dark at 4 °C to block non-specific binding sites for antibodies. The following antibodies were used for fluorescent staining: PerCP anti-mouse Ly-6G (0.25 μg/10^6 cells), FITC Anti-mouse F4/80 (0.25 μg/10^6 cells). Cells were incubated with antibodies for 1 h in the dark at 4 °C, washed with PBS to remove excessive antibody and suspended in cell staining buffer to perform flow cytometry analysis. The viability of the cellular suspension was determined through propidium iodide (PI) staining as above indicated. Only PI^{-ve} cells were included in the analysis. Samples were analysed using InCyte™ software (Merck Millipore, Darmstadt, Germany). Neutrophils were defined as Ly-$6G^+F4/80^-$ cells and their number was determined per ml of peritoneal lavage.

7.4. Materials

TNBS, DSS, zymosan A, dexamethasone, ethanol, HTAB, 30% hydrogen peroxide, tetramethylbenzidine were purchased from Sigma Aldrich™ (St. Louis, MO). PerCP anti-mouse Ly-6G, FITC anti-mouse F4/80, propidium iodide were purchased from BioLegend™ (San Diego, CA, USA), and IgG1-Fc from Millipore™ (Merck, Darmstadt, Germany). Drugs were dissolved in saline solution containing DMSO 1% the day of the experiment.

7.5. Statistics

All data were presented as mean ± SEM. Comparison among experimental groups were made using analysis of variance (one-way or two-way ANOVA) followed by Bonferroni's post-test, when $P < 0.05$, chosen as level of statistical significance, was achieved. Non-parametric Kruskal-Wallis analysis, followed by Dunn's post-test, was applied for statistical comparison of MS. All analyses were performed using Prism 9 software (GraphPad Software Inc. San Diego, CA, USA).

Author contributions

The manuscript was written by M.R. and S.B. through contributions of all authors, who have given approval to the final version of the manuscript.

Declaration of competing interest

The authors declare that they have no known competing financial interests or personal relationships that could have appeared to influence the work reported in this paper.

Data availability

Data will be made available on request.

Acknowledgment

Q4) Have we correctly interpreted the following funding sources and country names you cited in your article? COST, Belgiu,; University of Parma, Italy; FNRS, Belgium; Luxembourg Institute of Health (LIH), Belgium; Luxembourg National Research Fund, Belgium?

This work was supported by the University of Parma and by the European Crohn's and Colitis Organisation (to S.B. and M.R.), the Luxembourg Institute of Health (LIH) and Luxembourg National Research Fund (INTER/FNRS/20/15084569 to A.C. and M.S.) and FNRS Télévie (7.8508.22, 7.8504.20 and 7.4593.19 to A.C. and M.S). M.S, A.C., and M.R. are members of the COST Action CA 18133 "European Research Network on Signal Transduction—ERNEST". Prof. Federica Vacondio is also acknowledged for helpful discussion and interactions.

Appendix A. Supplementary data

Supplementary data to this article can be found online at https://doi.org/10.1016/j.ejmech.2022.114703.

References

[1] W.Y. Lai, A. Mueller, Latest update on chemokine receptors as therapeutic targets, Biochem. Soc. Trans. 49 (2021) 1385–1395.
[2] R. Solari, J.E. Pease, M. Begg, Chemokine receptors as therapeutic targets: why aren't there more drugs? Eur. J. Pharmacol. 746 (2015) 363–367.
[3] D.P. Dyer, Understanding the mechanisms that facilitate specificity, not redundancy, of chemokine-mediated leukocyte recruitment, Immunology 160 (2020) 336–344.
[4] E. Schutyser, S. Struyf, J. Van Damme, The CC chemokine CCL20 and its receptor CCR6, Cytokine Growth Factor Rev. 14 (2003) 409–426.
[5] I. Comerford, M. Bunting, K. Fenix, S. Haylock-Jacobs, W. Litchfield, Y. Harata-Lee, M. Turvey, J. Brazzatti, C. Gregor, P. Nguyen, E. Kara, S.R. McColl, An immune paradox: how can the same chemokine axis regulate both immune tolerance and activation?: CCR6/CCL20: a chemokine axis balancing immunological tolerance and inflammation in autoimmune disease, Bioessays 32 (2010) 1067–1076.
[6] N. Kulkarni, H.T. Meitei, S.A. Sonar, P.K. Sharma, V.R. Mujeeb, S. Srivastava, R. Boppana, G. Lal, CCR6 signaling inhibits suppressor function of induced-Treg during gut inflammation, J. Autoimmun. 88 (2018) 121–130.
[7] H.T. Meitei, N. Jadhav, G. Lal, CCR6-CCL20 axis as a therapeutic target for autoimmune diseases, Autoimmun. Rev. 20 (2021) 102846.
[8] C. Abraham, J.H. Cho, Inflammatory bowel disease, N. Engl. J. Med. 361 (2009) 2066–2078.
[9] H.K. Skovdahl, A. van B. Granlund, A.E. Østvik, T. Bruland, I. Bakke, S.H. Torp, J.K. Damås, A.K. Sandvik, Expression of CCL20 and its corresponding receptor CCR6 is enhanced in active inflammatory bowel disease, and TLR3 mediates CCL20 expression in colonic epithelial cells, PLoS One 10 (2015) e0141710.
[10] H.K. Skovdahl, J.K. Damås, A. van B. Granlund, A.E. Østvik, B. Doseth, T. Bruland, T.E. Mollnes, A.K. Sandvik, C-C motif ligand 20 (CCL20) and C-C motif chemokine receptor 6 (CCR6) in human peripheral blood mononuclear cells: dysregulated in ulcerative colitis and a potential role for CCL20 in IL-1β release, Int. J. Mol. Sci. 19 (2018) E3257.
[11] A. Kaser, O. Ludwiczek, S. Holzmann, A.R. Moschen, G. Weiss, B. Enrich, I. Graziadei, S. Dunzendorfer, C.J. Wiedermann, E. Mürzl, E. Grasl, Z. Jasarevic, N. Romani, F.A. Offner, H. Tilg, Increased expression of CCL20 in human inflammatory bowel disease, J. Clin. Immunol. 24 (2004) 74–85.
[12] J.Z. Liu, S. van Sommeren, H. Huang, S.C. Ng, R. Alberts, A. Takahashi, S. Ripke, J.C. Lee, L. Jostins, T. Shah, S. Abedian, J.H. Cheon, J. Cho, N.E. Dayani, L. Franke, Y. Fuyuno, A. Hart, R.C. Juyal, G. Juyal, W.H. Kim, A.P. Morris, H. Poustchi, W.G. Newman, V. Midha, T.R. Orchard, H. Vahedi, A. Sood, J.Y. Sung, R. Malekzadeh, H.-J. Westra, K. Yamazaki, S.-K. Yang, Association analyses identify 38 susceptibility loci for inflammatory bowel disease and highlight shared genetic risk across populations, International Multiple Sclerosis Genetics Consortium, International IBD Genetics Consortium, J.C. Barrett, B.Z. Alizadeh, M. Parkes, T. Bk, M.J. Daly, M. Kubo, C.A. Anderson, R.K. Weersma. Nat. Genet. 47 (2015) 979–986.
[13] K. Katchar, C.P. Kelly, S. Keates, M.J. O'brien, A.C. Keates, MIP-3alpha neutralizing monoclonal antibody protects against TNBS-induced colonic injury and inflammation in mice, Am. J. Physiol. Gastrointest. Liver Physiol. 292 (2007) G1263–G1271.
[14] R. Varona, V. Cadenas, J. Flores, C. Martínez-A, G. Márquez, CCR6 has a non-redundant role in the development of inflammatory bowel disease, Eur. J. Immunol. 33 (2003) 2937–2946.
[15] I. Marafini, I. Monteleone, V. Dinallo, D. Di Fusco, V. De Simone, F. Laudisi, M.C. Fantini, A. Di Sabatino, F. Pallone, G. Monteleone, CCL20 is negatively regulated by TGF-β1 in intestinal epithelial cells and reduced in crohn's disease patients with a successful response to mongersen, a Smad7 antisense oligonucleotide, J Crohns Colitis 11 (2017) 603–609.
[16] D. Currò, D. Pugliese, A. Armuzzi, Frontiers in drug Research and development for inflammatory bowel disease, Front. Pharmacol. 8 (2017) 400.
[17] Y. Li, J. Chen, A.A. Bolinger, H. Chen, Z. Liu, Y. Cong, A.R. Brasier, I.V. Pinchuk, B. Tian, J. Zhou, Target-based small molecule drug discovery towards novel therapeutics for inflammatory bowel diseases, Inflamm. Bowel Dis. 27 (2021) S38–S62.
[18] R. Bai, X. Jie, C. Yao, Y. Xie, Discovery of small-molecule candidates against inflammatory bowel disease, Eur. J. Med. Chem. 185 (2020) 111805.
[19] T. Tawaraishi, N. Sakauchi, K. Hidaka, K. Yoshikawa, T. Okui, H. Kuno, I. Chisaki, K. Aso, Identification of a novel series of potent and selective CCR6 inhibitors as biological probes, Bioorg. Med. Chem. Lett. 28 (2018) 3067–3072.
[20] D. Dairaghi, D. R. Dragoli, J. Kalisiak, C. W. Lange, M. R. Leleti, Y. Li, R. M. Lui, V. R. Mali, V. Malathong, J. P. Powers, H. Tanaka, J. Tan, M. J. Walters, J. Yang, P. Zhang, Ccr6 Compounds, WO2015/084842.
[21] C. D. Hein, T. T. Duong, S. Sinha, L. Li, J. H. Nguyen, D. W. Old, R. Burk, V. Viswanath, S. Rao, J. E. Donello, 3,4-disubstituted 3-Cyclobutene-1,2-Diones and Use Thereof, US2019/0047947.
[22] J. J. Campbell, K. Ebsworth, A. Krasinski, V. R. Mali, J. Mcmahon, R. Singh, J. Yang, C. Yu, P. Zhang, Methods of Treating Generalized Pustular Psoriasis with an Antagonist of Ccr6 or Cxcr2, WO2019/136370.
[23] O. Allemann, E. Caroff, A. Chavanton-Arpel, A. Croxford, F. Hubler, L. Jacob, E. Meyer, S. Richard-Bildstein, Azetidin-3-ylmethanol Derivatives as Ccr6 Receptor Modulators, WO2021/219849.
[24] J.G. Moffat, J. Rudolph, D. Bailey, Phenotypic screening in cancer drug discovery - past, present and future, Nat. Rev. Drug Discov. 13 (2014) 588–602.
[25] D.J. Wasilko, Z.L. Johnson, M. Ammirati, Y. Che, M.C. Griffor, S. Han, H. Wu, Structural basis for chemokine receptor CCR6 activation by the endogenous protein ligand CCL20, Nat. Commun. 11 (2020) 3031.
[26] C. Munk, V. Isberg, S. Mordalski, K. Harpsøe, K. Rataj, A.S. Hauser, P. Kolb, A.J. Bojarski, G. Vriend, D.E. Gloriam, GPCRdb: the G protein-coupled receptor database - an introduction, Br. J. Pharmacol. 173 (2016) 2195–2207.
[27] P. Vincetti, A. Brianza, N. Scalacci, G. Costantino, D. Castagnolo, M. Radi, A microwave-assisted multicomponent protocol for the synthesis of benzofuran-2-carboxamides, Tetrahedron Lett. 57 (2016) 1464–1467.
[28] S. Tassini, D. Castagnolo, N. Scalacci, M. Kissova, J.I. Armijos-Rivera, F. Giagnorio, G. Maga, G. Costantino, E. Crespan, M. Radi, A multicomponent pharmacophore fragment-decoration approach to identify selective LRRK2-targeting probes, MedChemComm 7 (2016) 484–494.
[29] A. Schüller, V. Hahnke, G. Schneider, SmiLibv2.0:ajava-based tool for rapid combinatorial library lnumeration, QSAR Comb. Sci. 26 (2007) 407–410.
[30] G.L. Warren, C.W. Andrews, A.-M. Capelli, B. Clarke, J. LaLonde, M.H. Lambert, M. Lindvall, N. Nevins, S.F. Semus, S. Senger, G. Tedesco, I.D. Wall, J.M. Woolven, C.E. Peishoff, M.S. Head, A critical assessment of docking programs and scoring functions, J. Med. Chem. 49 (2006) 5912–5931.
[31] M.M. Rosenkilde, T. Benned-Jensen, T.M. Frimurer, T.W. Schwartz, The minor binding pocket: a major player in 7TM receptor activation, Trends Pharmacol. Sci. 31 (2010) 567–574.
[32] P.J. Trivedi, D.H. Adams, Chemokines and chemokine receptors as therapeutic targets in inflammatory bowel disease; pitfalls and promise, Journal of Crohn's and Colitis 12 (2018) S641–S652.
[33] S.G. Kang, R.J. Piniecki, H. Hogenesch, H.W. Lim, E. Wiebke, S.E. Braun, S. Matsumoto, C.H. Kim, Identification of a chemokine network that recruits FoxP3+ regulatory T cells into chronically inflamed intestine, Gastroenterology 132 (2007) 966–981.
[34] H. Wen, C.M. Hogaboam, N.W. Lukacs, D.N. Cook, S.A. Lira, S.L. Kunkel, The chemokine receptor CCR6 is an important component of the innate immune response, Eur. J. Immunol. 37 (2007) 2487–2498.
[35] R. Robert, C. Ang, G. Sun, L. Juglair, E.X. Lim, L.J. Mason, N.L. Payne, C.C.A. Bernard, C.R. Mackay, Essential role for CCR6 in certain inflammatory diseases demonstrated using specific antagonist and knockin mice, JCI Insight 2 (2017) e94821.
[36] G. Bouma, S. Zamuner, K. Hicks, A. Want, J. Oliveira, A. Choudhury, S. Brett, D. Robertson, L. Felton, V. Norris, D. Fernando, M. Herdman, R. Tarzi, CCL20 neutralization by a monoclonal antibody in healthy subjects selectively inhibits recruitment of CCR6 + cells in an experimental suction blister: CCL20 inhibition selectively prevents CCR6 + T-cell recruitment, Br. J. Clin. Pharmacol. 83 (2017) 1976–1990.
[37] M. Veny, A. Fernández-Clotet, J. Panés, Controlling leukocyte trafficking in IBD, Pharmacol. Res. 159 (2020) 105050.
[38] P. Kiesler, I.J. Fuss, W. Strober, Experimental models of inflammatory bowel diseases, Cell Mol Gastroenterol Hepatol 1 (2015) 154–170.
[39] J.L. Cash, G.E. White, D.R. Greaves, Chapter 17. Zymosan-induced peritonitis as a simple experimental system for the study of inflammation, Methods Enzymol. 461 (2009) 379–396.
[40] T.A. Halgren, MMFF VI. MMFF94s option for energy minimization studies, J. Comput. Chem. 20 (1999) 720–729.
[41] W.J. Geldenhuys, K.E. Gaasch, M. Watson, D.D. Allen, C.J. Van der Schyf, Optimizing the use of open-source software applications in drug discovery, Drug Discov. Today 11 (2006) 127–132.

[42] O. Trott, A.J. Olson, AutoDock Vina, Improving the speed and accuracy of docking with a new scoring function, efficient optimization, and multithreading, J. Comput. Chem. 31 (2010) 455–461.
[43] S. Dallakyan, A.J. Olson, Small-molecule library screening by docking with PyRx, Methods Mol. Biol. 1263 (2015) 243–250.
[44] The PyMOL Molecular Graphics System, Version 1.5.0.4 Schrödinger, LLC.
[45] R. Luís, G. D'Uonnolo, C.B. Palmer, M. Meyrath, T. Uchański, M. Wantz, B. Rogister, B. Janji, A. Chevigné, M. Szpakowska, Nanoluciferase-based methods to monitor activation, modulation and trafficking of atypical chemokine receptors, Methods Cell Biol. 169 (2022) 279–294.
[46] G. D'Uonnolo, N. Reynders, M. Meyrath, D. Abboud, T. Uchański, T. Laeremans, B.F. Volkman, B. Janji, J. Hanson, M. Szpakowska, A. Chevigné, The extended N-terminal domain confers atypical chemokine receptor properties to CXCR3-B, Front. Immunol. 13 (2022) 868579.
[47] M. Meyrath, M. Szpakowska, J. Zeiner, L. Massotte, M.P. Merz, T. Benkel, K. Simon, J. Ohnmacht, J.D. Turner, R. Krüger, V. Seutin, M. Ollert, E. Kostenis, A. Chevigné, The atypical chemokine receptor ACKR3/CXCR7 is a broad-spectrum scavenger for opioid peptides, Nat. Commun. 11 (2020) 3033.
[48] Q. Wan, N. Okashah, A. Inoue, R. Nehmé, B. Carpenter, C.G. Tate, N.A. Lambert, Mini G protein probes for active G protein-coupled receptors (GPCRs) in live cells, J. Biol. Chem. 293 (2018) 7466–7473.
[49] M.J. Waldner, M.F. Neurath, Chemically induced mouse models of colitis, Curr Protoc Pharmacol. Chapter 5 (2009) Unit 5.55.
[50] H.S. Cooper, S.N. Murthy, R.S. Shah, D.J. Sedergran, Clinicopathologic study of dextran sulfate sodium experimental murine colitis, Lab. Invest. 69 (1993) 238–249.
[51] C.L. Ivey, F.M. Williams, P.D. Collins, P.J. Jose, T.J. Williams, Neutrophil chemoattractants generated in two phases during reperfusion of ischemic myocardium in the rabbit. Evidence for a role for C5a and interleukin-8, J. Clin. Invest. 95 (1995) 2720–2728.
[52] S.D. Moore-Olufemi, R.A. Kozar, F.A. Moore, N. Sato, H.T. Hassoun, C.S. Cox, B.C. Kone, Ischemic preconditioning protects against gut dysfunction and mucosal injury after ischemia/reperfusion injury, Shock 23 (2005) 258–263.